Available online at www.sciencedirect.com
ScienceDirect
European Journal of Medicinal Chemistry 44 (2009) 42–53
EUROPEAN JOURNAL OF MEDICINAL CHEMISTRY
http://www.elsevier.com/locate/ejmech

Original article

'Sum of activities' as dependent parameter: A new CoMFA-based approach for the design of pan PPAR agonists

Sandeep Sundriyal, Prasad V. Bharatam*

Department of Medicinal Chemistry, National Institute of Pharmaceutical Education and Research (NIPER), Phase X, S.A.S. Nagar, Mohali 160 062, Punjab, India

Received 24 October 2007; received in revised form 4 March 2008; accepted 6 March 2008
Available online 28 March 2008

Abstract

A 'sum-model' (3D QSAR − CoMFA) has been developed to design PPAR$_{\alpha/\gamma/\delta}$ (peroxisome proliferator activated receptor) pan agonists by using the sum of activities (EC_{50}) of compounds against individual subtypes as a dependent parameter. In addition, the three subtype specific CoMFA models were also generated using the identical training set molecules ($N = 28$). All four models were validated using the popular 'leave-one-out' (LOO) method and with a test set of 9 molecules. The generated models were found to be statistically significant with $r^2_{cv} > 0.5$ and $r^2_{ncv} > 0.9$ and the lower values of standard error of estimation (SEE) ranging from 0.097 to 0.160. From the contour map analyses the 'sum-model' was found to represent the three subtype specific models and also predicted the sum of activities of the training set molecules with reasonable accuracy. The new molecules were designed based on the 'sum-model' and were found to dock well in the PPARγ active site. This approach may find wider applications in the research related to other classes of 'designed multiple ligands'.

Keywords: PPAR; Pan agonists; Designed multiple ligands; QSAR; CoMFA; Type 2 diabetes; Docking

1. Introduction

Peroxisome proliferator activated receptor (PPAR) is an important subclass of nuclear hormone receptor (NHR) super family of ligand dependent transcription factors [1]. To date, three isotypes of PPAR family, PPARγ, PPARα and PPARβ/δ, have been recognized, and found to play an important role in carbohydrate and lipid metabolism [2]. These subtypes have distinct pattern of tissue distribution and different pharmacological roles depending on the cell type. These receptors undergo a conformational change upon binding to a natural or synthetic ligand and form a heterodimer with retinoid X receptor (RXR). The resultant heterodimer binds to peroxisome proliferator response element (PPRE) in the promoter region of the target genes leading to the transcription of the genes. In addition, a variety of cofactors (coactivators/corepressors) are recruited which have the ability to initiate or suppress the transcription process. This biological mechanism of PPARs is well described in a recent review by Kota et al. [3].

Out of the various isoforms, PPARγ is the most studied one for the drug discovery purpose. Rosiglitazone and pioglitazone (**1**, **2**; Fig. 1) are the currently marketed PPARγ activators used for the treatment of type 2 diabetes [4,5]. However, side effects like weight gain, fluid retention, oedema, increased heart weight of rodents, etc. are the issues of major concern for these agents thus limiting their general clinical use [6]. PPARα selective agonists such as fenofibrate and clofibrate (**4**, **5**; Fig. 1) are known to increase the disposal of glucose to liver from the peripheral tissues (muscles and adipose tissues) and are used clinically to treat dyslipidemia [7,8]. Thus, the dual PPARα/γ agonists were envisaged for the treatment of insulin resistance [9,10]. Though some of the dual PPARα/γ agonists, such as KRP-297, tesaglitazar, ragaglitazar and muraglitazar (**5**–**8**; Fig. 1) showed promising results, they were discontinued due to toxicity problems in animal models.

* Corresponding author. Tel.: +91 172 2214684.
E-mail address: pvbharatam@niper.ac.in (P.V. Bharatam).

0223-5234/$ - see front matter © 2008 Elsevier Masson SAS. All rights reserved.
doi:10.1016/j.ejmech.2008.03.014

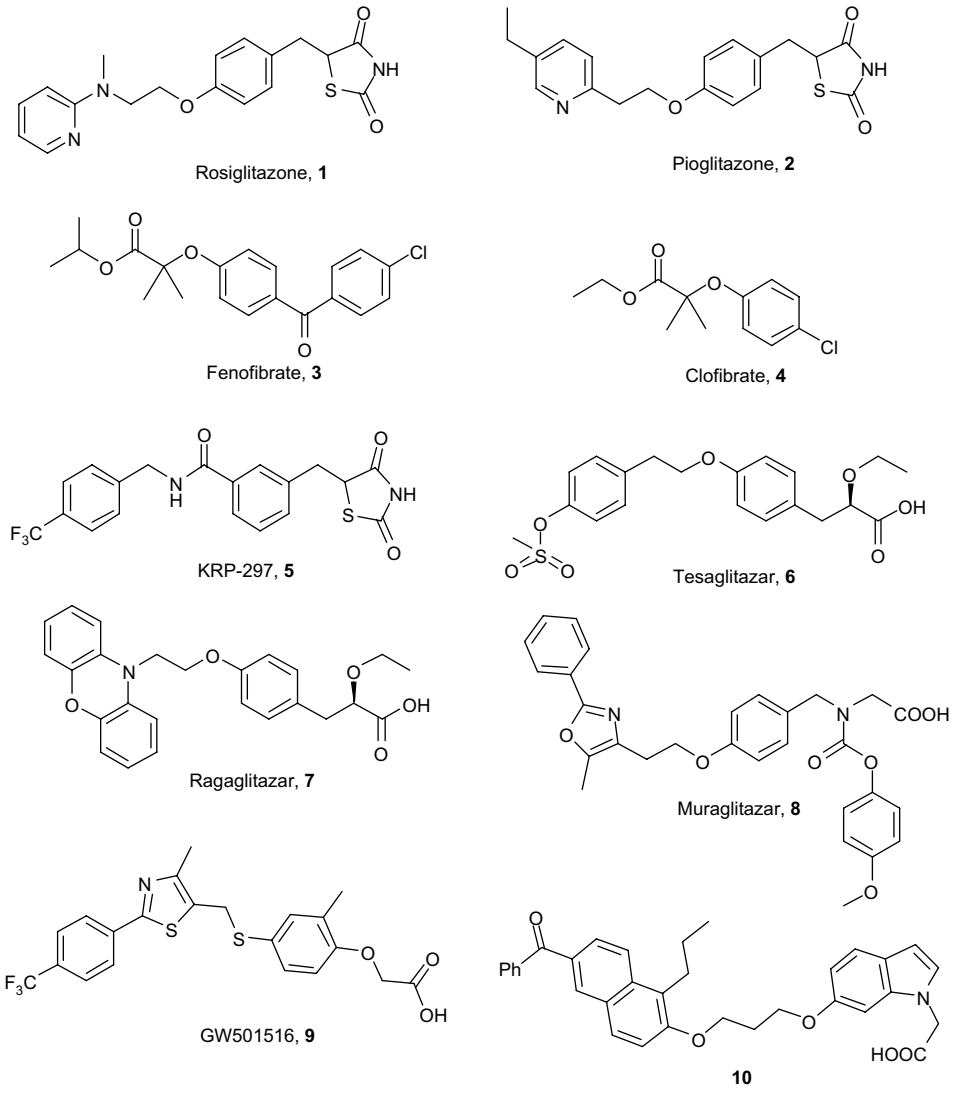

Fig. 1. Structures of some known selective, dual and pan PPAR agonists.

Recently, role of third isoform of PPAR, that is PPARδ, is beginning to emerge. Various studies have proposed the pharmacological role for this subtype in cholesterol and lipid homeostasis. Selective activation of PPARδ with the synthetic ligand GW501516 (**9**; Fig. 1) is shown to be associated with improved insulin sensitivity, prevention of weight gain and elevated high-density lipoproteins (HDL) and other effects related to lipid metabolism [11–17]. Thus, discovering a molecule that can simultaneously activate the three isoforms of PPAR might be an exciting venture for a medicinal chemist concerned with drug discovery related to diabetes, obesity and related metabolic disorders. Many pharmaceutical companies have already initiated efforts in this direction and as a result various reports have emerged in literature that describes the design and synthesis of such molecules generally termed as PPAR pan agonists [18–22]. The animal studies have validated the concept and these agents are shown to have improved pharmacological profiles over selective PPARγ or dual PPARα/γ agonists. One of the PPAR pan agonists, PLX204 (PPM-204), has reached the phase 2 of clinical trials [23,24].

PPAR pan agonists are a type of designed multiple ligands [25], which act on multiple macromolecular targets with similar binding pockets. However, designing such molecules is a daunting task as fine tuning of substituents is required to obtain the optimum potency at all three subtypes of PPARs. It is possible that one substituent at a particular position may be favorable for activity at one subtype but detrimental for the activity for other subtype. Thus, in order to obtain optimum biological activity at all three subtypes, such effects have to be quantified. Recently, scientists at Bayer HealthCare, have provided extensive synthetic and biological studies on a series of pan agonists based on indanylacetic acid derivatives [17]. The substituent effect at three positions in the lipophilic tail portion was studied (Table 1). Results show that the activity at three subtypes can be fine tuned by varying substituents at these positions. In particular, absence of any substituent at R_1 position led to poor activity at PPARα and PPARγ subtype

Table 1
In vitro activities of 4-thiazolylphenyl analogs as described in Ref. [18] (all the compound numbers are kept same as in the original reference)

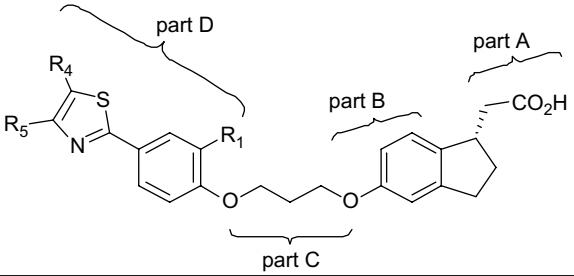

Compd	R^4	R^5	R^1	*h*PPARα EC_{50} (nM)	*h*PPARδ EC_{50} (nM)	*h*PPARγ EC_{50} (nM)	Sum of activities EC_{50} (nM)
34a	H	H	*n*-Pr	111	1.6	48	160.6
34b	H	H	OMe	255	0.58	374	629.6
34c	H	Me	OMe	268	2.7	960	1230.7
34d	H	Et	H	1280	4.4	874	2158.4
34e	H	Et	*n*-Pr	147	11	45	203.0
34f	H	Et	OMe	254	2.5	65	321.5
34g	H	*t*-Bu	*n*-Pr	87	11	18	116.0
34h	H	CF_3	*n*-Pr	197	3.3	55	255.3
34i	H	CF_3	OMe	437	2.9	327	766.9
34j	Me	Me	H	1250	2.9	280	1532.9
34k	Me	Me	OMe	83	4	33	120.0
34l			H	112	1.3	1200	1313.3
34m			*n*-Pr	328	3.5	94	425.5
34n			OMe	53	4.1	116	173.1
34o			H	391	2.2	294	687.2
34p			*n*-Pr	43	1.9	12	56.9
34q			OMe	44	3.3	84	131.3
34r			*n*-Pr	101	4.0	42	147.0
34s			OMe	328	1.3	181	510.3
34t			OMe	526	5.2	214	745.3
34u	$COCH_3$	Me	H	2530	6.9	480	3016.9
34v	$COCH_3$	Me	*n*-Pr	175	18	17	210.0
34w	$COCH_3$	Me	OMe	560	3.4	49	612.4
34x	$CONMe_2$	Me	*n*-Pr	140	4.4	20	164.4
34y	$CONMe_2$	Me	OMe	803	2.1	–	–
34z	COOH	Me	H	10,000	218	312	10,530.0
34aa	COOH	Me	*n*-Pr	1690	46	238	1974.0
34ab	COOH	Me	OMe	10,000	28	1000	11,028.0
34ac	COOH	CH_2OH	*n*-Pr	6490	12	891	7393.0
34ad	H	CH_2CO_2H	*n*-Pr	2480	4.6	27	2511.6
34ae	H	OMe	H	5800	1.3	300	6101.3
34af	H	OMe	OMe	755	3.0	69	827.0
34ag	H	OEt	H	100	1.2	753	854.2
34ah	H	OEt	*n*-Pr	105	2	41	148.0
34ai	H	OEt	OMe	1350	3.4	920	2273.4
34aj	H	O*i*-Pr	*n*-Pr	47	2.3	45	94.3
34ak	H	O*i*-Pr	OMe	180	3	44	227.0
34al	Me	OEt	*n*-Pr	61	3.2	34	98.2
34am	Me	OEt	OMe	150	6	177	333.0
34an	Et	OEt	OMe	520	5.4	362	887.4

but maintains potency at PPARδ. Moreover, most of the compounds were found to have potent activity at PPARδ but possessed moderate EC_{50} for PPARα and PPARγ subtype. It should be noted that even though **34r** has higher EC_{50} (poor activity) values in vitro on all the subtypes as compared to **34p**, it possessed good in vivo profile than the later. This may be due to various reasons such as better bioavailability of **34r** over **34p**, but shows that a molecule possessing comparable in vitro profile to **34r** may be a good candidate for further screening. Thus, the goal should be not only to design molecules that have in vitro activities comparable to **34p** or **34r** at all the receptor subtypes, but also the activity is required to be improved for a subtype where most of the molecules are lagging, that is PPARα and PPARγ.

Comparative molecular field analysis (CoMFA) is one of the widely used 3D QSAR methods that is used for predicting structure activity/property relationship. It is based on the calculated energies of steric and electrostatic interactions between the compound and the probe atom placed at the various intersections of a regular 3-D lattice. Thus, a structure activity relationship is developed by using partial least squares (PLS) analysis, a powerful statistical tool. The results are obtained in the form of steric and electrostatic contour maps which guide about the potential regions of the molecule in 3-D space that should be modified in order to optimize biological activity.

For the design of PPAR pan agonists, CoMFA models for the individual subtype may not be helpful as they would provide information about optimizing the activity for that particular subtype and overall picture may not be clear. Thus a combined model is required that should have balanced fields with respect to biological activities at all the three receptor subtypes. Such a problem can be dealt by manipulating the biological activities to generate a new value that can be used to develop a 'hybrid-model' which differs from the one generated from the original biological activities and carries new information. This is possible because biological activities and electrostatic and steric fields around a molecule are correlated. Thus, different fields of a molecule may be responsible for exhibiting two different biological activities due to the involvement of different receptors. When these biological activities are manipulated, a corresponding hybridization of fields should be observed that can provide useful information.

The selectivity issues have been studied by many workers using this approach. For example, when a set of ligands show activity towards two receptors the ratio of activities (K_i or IC_{50}, etc.) is used to build the selectivity model. Wong et al. studied the structural requirement for the selective ligand binding to diazepam-insensitive benzodiazepine receptors [26]. Similarly, Baskin et al. addressed the selectivity issue of ligands acting on both glycine/NMDA and AMPA receptors, by using the difference of pK_i ($-\log K_i$) for the two receptors (equivalent to division of K_i values) [27]. On similar lines we introduced the concept of 'additivity of fields' for the design of PPARα/γ dual activators, where the pIC_{50} ($-\log IC_{50}$) values against two receptor subtypes were added (equivalent to multiplication of IC_{50} values) to give a 'dual-model' possessing the characteristics of both individual α- and γ-models [28]. We have also extended the concept of 'selectivity fields' for the study of molecules acting simultaneously on glycogen synthase kinase 3 (GSK3) and cyclin dependent kinases such as CDK2 and CDK4 [29]. As apparent from these examples, careful manipulation of activities may lead to the corresponding hybridization of molecular fields associated with the molecules and gets reflected quantitatively in the final model. However, the kind of manipulation required should be done according to problem in hand.

In this particular case of PPAR pan agonists, it was realized that a CoMFA model is desired that should (i) possess the balanced fields of all the subtypes and (ii) also should closely match the model of a subtype where most of the molecules show poor activity (PPARα and PPARγ in this case). It was reasoned that the sum of activities (EC_{50}) at all the subtypes for the molecules should be appropriate for this purpose. The addition would lead to a new value that should be closer to the one that is largest (representing poor EC_{50}), and would represent it more closely. For instance, in case of **34z** the sum of activities at all the subtypes is 10,530 nM, (Table 1; last column) which is closer to the EC_{50} against PPARα that is 10,000 nM. Similarly, for **34ab** total sum is 11,028 nM that is also close to EC_{50} for PPARα subtype that is, 10,000 nM. Thus, if CoMFA model is built using these sum values as dependent parameter a corresponding 'sum-model' should be obtained with balanced fields of all the individual models and should be more similar to PPARα and PPARγ-model rather than the PPARδ. This should allow the design of molecules with balanced activity at all the subtypes together with the scope of improving the activity particularly at PPARα and PPARγ subtypes.

In order to validate this hypothesis, individual α-, δ- and γ-CoMFA models together with the 'sum-model' were developed, using the dataset of the given compounds (Table 1). This was a challenging task given that the previously reported attempts to develop QSAR models for PPAR agonists using transactivation data (EC_{50}) led to poor models [30,31]. On the other hand, good QSAR models are reported using binding affinity (K_i or IC_{50}) data as dependent parameters [28,30–35]. It should be noted that K_i or IC_{50} data in this case only represent the binding strength of a compound for the receptor, while EC_{50} values represents true biological activity in true sense as it would also confirm whether the compound is a agonist or antagonist. Thus, the models derived from EC_{50} data should have greater value as it would predict the agonistic property of a molecule towards the PPAR receptor.

2. Materials and methods

2.1. Dataset

A dataset consisting of a series of indylacetic acid derivatives carrying 4-thiazloyl-phenoxy tail groups, acting as pan PPAR agonists [17] (Table 1) was selected to develop four CoMFA models: (i) α-model, (ii) δ-model, (iii) γ-model and (iv) 'sum-model' (based on sum of EC_{50} at all three subtypes). These molecules are composed of four parts: part A constitutes the acidic fragment, part B refers to the phenoxy ring next to the acidic fragment, part C is composed of a $(CH_2)_n$ linker and the last part D is composed of 4-thiazolyl phenoxy tail group. One of the molecules, **34y** was dropped from the dataset as activity for PPARγ is not reported for this molecule. Thus, the dataset of 39 molecules was sorted randomly into training set and test set comprising of 28 and 11 molecules, respectively, in the process of model refinement for all four CoMFA models reported herein. The biological activities have been reported as the EC_{50} values in nanomolar scale (nM) using in vitro assays for all three subtypes as described in original reference by Rudolph et al. [17]. These values were converted to pIC_{50} ($-\log IC_{50}$) values in molar terms and are used as the dependent variables in the CoMFA analysis (Table 3 and 4). For the 'sum-model' EC_{50} values against all the subtypes were added and converted to pIC_{50} values in a similar way.

2.2. Minimization and alignment

The ligands under study were built employing the SKETCH module of the SYBYL6.9 molecular modeling package [36] installed on a Silicon Graphics Octane2 workstation with IRIX 6.5 operating system. Although bioactive conformation of the given set of molecules is not known, these molecules are structurally very similar to indole class of pan agonist **10** (Fig. 1), crystal structure for which is available with PPARγ (PDB code 2F4B) [20]. We assumed that both classes of molecules should share the similar conformation in the active site of the receptor due to similar structure. This assumption is based on a recent study conducted on all the protein crystal structures with resolution greater than 2.5 Å, available in the protein databank (PDB) [37]. From this study it could be concluded that the structurally similar molecules bind similarly to a target. Thus the most active molecule **34p**, having the least 'sum-EC_{50}' value, was built upon the co-crystallized ligand extracted from 2F4B (**10**; Fig. 1) and minimized using PM3 method while maintaining the U-shape of ligands, essential for activity [38]. The rest of the molecules were built taking **34p** as the template and changing the required substituents for the subsequent set of molecules and minimized similarly. MOPAC charges [39] were assigned to all the molecules. The alignment of molecules was done using the common substructure of 25 atoms (as shown in red below) using database alignment option in SYBYL6.9. Fig. 2 depicts the aligned training set molecules.

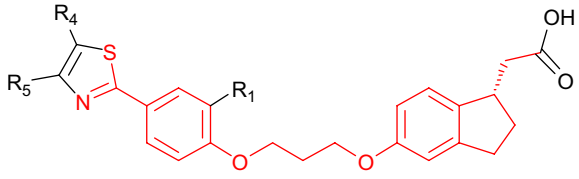

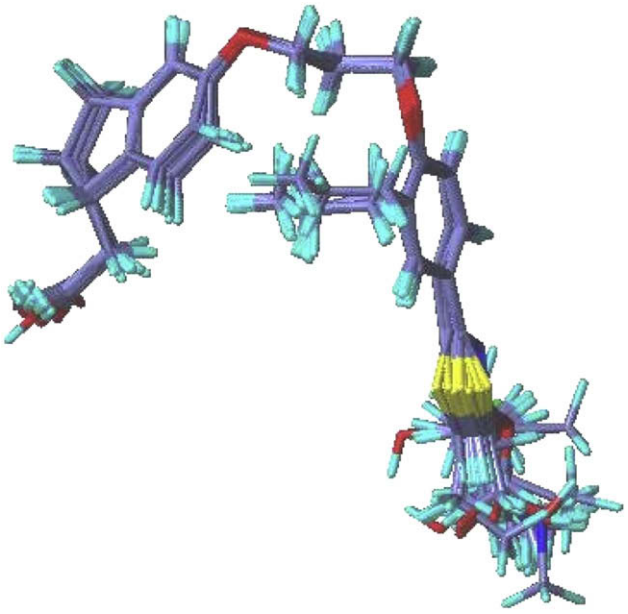

Fig. 2. Aligned training set molecules.

2.3. CoMFA 3D QSAR models

The standard Tripos settings were used to carry out the CoMFA analysis. To derive the CoMFA fields, a 3D cubic lattice was created; the steric and electrostatic parameters were calculated at each lattice intersection of regularly spaced grid of 2.0 Å in all three dimensions within the defined region. The van der Waals potential and the Coulombic term representing the steric and electrostatic fields were calculated using standard Tripos force fields. An sp^3 carbon atom with a positive charge (+1) was used as a probe atom to generate steric (Lennard–Jones potential) field energies and electrostatic (Coulombic potential) field energies. A distance dependent dielectric constant of 1.00 was used. The steric and electrostatic fields were truncated at +30.00 kcal/mol.

2.4. Partial least squares (PLS)

This statistical method was used to linearly correlate the CoMFA fields to the binding affinity values. The cross-validation analysis was performed using leave-one-out (LOO) method. The cross-validated r^2 (r^2_{cv}) that resulted in optimum number of components and lowest standard error of prediction were taken. Equal weights were assigned to steric and electrostatic fields using CoMFA_STD scaling option. To speed up the analysis and reduce noise, a minimum filter value σ of 2.00 kcal/mol was used. Final analysis was performed to calculate conventional r^2 (r^2_{ncv}) using the optimum number of components obtained from the cross-validation analysis. Cross-validation runs with varying number of groups were also performed to improve the confidence limits of the derived model. Since the statistical parameters were found to be the best for the model from the LOO method, it was employed for the predictions of the designed molecules.

2.5. Docking studies

Docking studies were carried out using the FlexX program [40] interfaced with SYBYL6.9. In this automated docking program, the flexibility of the ligands is considered while the protein or biomolecule is considered as a rigid structure. The ligand is built in an incremental fashion, where each new fragment is added in all possible positions and conformations to a pre-placed base fragment inside the active site. All the molecules for docking were sketched in the SYBYL and minimized using PM3 method and all the charges were removed. The 3D coordinates of the active sites were taken from the X-ray crystal structures of the PPARγ (PDB code 2F4B) reported as complex with the corresponding agonist (**10**) [20]. The active site was defined as the area within 6.5 Å around the co-crystallized ligand, and customization was done for the His423, Tyr473 and His449 so as to represent the reported H-bonding interactions. Formal charges were assigned to all the molecules and FlexX run was submitted.

3. Results and discussion

3.1. Statistical analysis

Four independent CoMFA models were built using the same training set: (i) α-model, based on the EC_{50} of the molecules towards PPARα as the dependent variable, (ii) γ-model, based on the EC_{50} of the molecules for the PPARγ receptor, (iii) δ-model, based on the EC_{50} of the molecules for the PPARδ receptor and (iv) 'sum-model', based on the sum of activities at all three subtypes. These CoMFA models were chosen after rigorous cycles of model-development and validation based on internal predictions of the training set and the external predictions of the test set. The statistical parameters for the three models developed are shown in Table 2. The sum-model shows the best statistical results with cross-validated r^2 (r^2_{cv}) = 0.757 with five components and noncross-validated r^2 (r^2_{ncv}) = 0.981 while the corresponding values for the other three models are 0.670 with five components and 0.969 for α-model, 0.555 with six components and 0.969 for δ-model and, 0.549 with five components and 0.941 for γ-model. Thus, these statistical parameters deny any possibility of chance correlation.

The fact that the 'sum-model' is closer to α- and γ-models can be observed from the difference in the contribution of steric and electrostatic fields of these models. The numerical value of this difference between sum-model and α-model is 1.8 (63.5–61.7 for steric or 36.5–38.3 for electrostatic fields) while the same difference for γ- and δ-model is 3.8 and 11.5, respectively. These values indicate that the 'sum-model' is closer to α-model, than to γ-model, and least similar to δ-model as expected.

The individual models (α-, δ- and γ-models) are expected to be useful for predicting the activity for the particular subtype while the 'sum-model' should predict the total sum of activity on all the three subtypes. In general, these models were found to be good at predicting the activities of the training and test set molecules, as shown in Table 3 and 4, respectively.

3.2. Contour analysis

In CoMFA method, results are presented as contour maps that correlate the change in biological activity with the molecular field values. The steric contour maps are represented in green and yellow colors while the electrostatic contours are depicted in red and blue colors. The green contours are indicative of favorable regions for sterically bulkier groups and the yellow contours are indicative of regions that are sterically less favorable. Similarly, the electrostatic red plots show the regions where the presence of a negative charge is expected to enhance the activity whereas the blue contours are indicative of regions where introducing or keeping positive charges are expected to improve the observed activity. Thus, these contour maps act as the guidance source to for the design of new molecules from the existing ones, with improved biological activity.

Table 2
PLS statistics of CoMFA models

Parameters	α-Model	δ-Model	γ-Model	Sum-model
No. of molecules in training set	28	28	28	28
No. of molecules in test set	9	9	9	9
r^2_{cv}	0.670	0.555	0.549	0.757
No. of components	5	6	5	5
r^2_{ncv}	0.969	0.969	0.941	0.981
SEE	0.141	0.108	0.160	0.097
F value	136.1	110.2	70.4	223.1
Steric field contributions	0.617	0.520	0.597	0.635
Electrostatic field contributions	0.383	0.480	0.403	0.365

The contour maps are limited to the regions where various substituents have been modified. These variations are mainly at the 4-thiazolyl phenoxy tail group (part D) where a variety of substituents (R_1, R_4 and R_5) have been tested. All the steric and electrostatic contour maps are mapped to the most active compounds (**34p** for α-, γ- and sum-model and **34b** for δ-model) and are shown in Figs. 3 and 4. (For interpretation of the references to color in text, the reader is referred to the web version of this article.) In case of α-model, the steric model (Fig. 3a) shows small green regions near the R_4 substituent of the thiazolyl ring and over the cyclohexyl ring, while yellow regions are scattered all over the tail portion. The δ-model (Fig. 3b) shows comparatively large sterically favorable region near and over the R_4 substituent. On the other hand γ-model shows (Fig. 3c) the green contours near the R_1 showing the importance of bulky group in this region. This observation is also in agreement to earlier reported findings of Sahoo and coworkers who reported that introduction of *n*-propyl group at this position increases the affinity of molecule for PPARγ subtype [41,42]. Similarly, Mahindroo et al. have also demonstrated that the presence of *n*-propyl group at this position in indole based molecules improved the activity in the functional assays [20]. However, there are only yellow contours all over the R_4 and R_5 showing steric bulk is disfavored around the thiazolyl ring. Interestingly, the 'sum-model' (Fig. 3d) shows the overall balance of all the individual models but is more closely matching the PPARα and PPARγ-models as expected. It shows small green regions near R_1 which represents the component of γ-model while a small green region over R_4 substituent may be a part of α- and δ-model. There are also yellow regions scattered all over the thiazolyl ring which are more or less similar to both α- and γ-models.

In case of electrostatic models also, the 'sum-model' looks similar to PPARα and PPARγ rather than PPARδ (Fig. 4a–d). It shows the presence of a blue contour near the R_4 while red one at the R_5 region which is similar to α-model in shape and size as expected. Additionally, a red contour can also be seen over the thiazolyl ring in all the cases. However, the red contour over the thiazolyl ring is broken in case of 'sum-model' as compared to α-model which is uniformly distributed. In addition, the 'sum-model' also shows some red contours near the carboxylic acid group which is also present in α- and γ-model but not in the δ-model. However, the electrostatic contours of δ-model are quite different from the 'sum-model' and only similarity is in the presence of blue contour near the R4 region. Thus, it can be concluded that the 'sum-model' possesses

Table 3
Actual (act) and predicted (pred) pIC_{50} values and the residuals (Δ) of the training set molecules for the α-, δ-, γ- and sum-model

Compd	Pred (α)	Act (α)	Δ	Pred (δ)	Act (δ)	Δ	Pred (γ)	Act (γ)	Δ	Pred (sum)	Act (sum)	Δ
34a	7.00	6.95	−0.05	8.82	8.80	−0.02	7.29	7.32	0.03	6.79	6.79	0.00
34b	6.65	6.59	−0.06	9.08	9.24	0.16	6.34	6.43	0.09	6.20	6.20	0.00
34c	6.50	6.57	0.07	8.67	8.57	−0.10	6.06	6.02	−0.04	5.97	5.91	−0.06
34d	5.64	5.89	0.25	8.42	8.36	−0.06	6.39	6.06	−0.33	5.55	5.66	0.11
34g	6.97	7.06	0.09	7.93	7.96	0.03	7.70	7.74	0.04	6.89	6.94	0.05
34h	6.67	6.70	0.03	8.40	8.48	0.08	7.27	7.26	−0.01	6.63	6.59	−0.04
34i	6.33	6.36	0.03	8.66	8.54	−0.12	6.32	6.49	0.17	6.05	6.12	0.07
34j	5.84	5.90	0.06	8.50	8.54	0.04	6.31	6.55	0.24	5.72	5.81	0.09
34l	6.95	6.95	0.00	8.94	8.89	−0.05	5.94	5.92	−0.02	5.85	5.88	0.03
34n	7.36	7.28	−0.08	8.39	8.39	0.00	6.97	6.94	−0.03	6.77	6.76	−0.01
34o	6.34	6.41	0.07	8.67	8.66	−0.01	6.43	6.53	0.10	6.07	6.16	0.09
34p	7.47	7.37	−0.10	8.68	8.72	0.04	7.99	7.92	−0.07	7.35	7.24	−0.11
34s	6.44	6.48	0.04	8.94	8.89	−0.05	6.86	6.74	−0.12	6.32	6.29	−0.03
34t	6.27	6.28	0.01	8.23	8.28	0.05	6.75	6.67	−0.08	6.19	6.13	−0.06
34u	5.84	5.60	−0.24	8.09	8.16	0.07	6.41	6.32	−0.09	5.61	5.52	−0.09
34v	6.54	6.76	0.22	7.83	7.74	−0.09	7.72	7.77	0.05	6.64	6.68	0.04
34z	5.05	5.00	−0.05	6.80	6.66	−0.14	6.32	6.51	0.19	4.93	4.98	0.05
34aa	5.51	5.77	0.26	7.41	7.34	−0.07	6.58	6.62	0.04	5.50	5.70	0.20
34ab	5.13	5.00	−0.13	7.31	7.55	0.24	6.38	6.00	−0.38	5.18	4.96	−0.22
34ac	5.24	5.19	−0.05	7.97	7.92	−0.05	6.06	6.02	−0.04	5.16	5.13	−0.03
34ad	5.80	5.61	−0.19	8.30	8.34	0.04	7.52	7.57	0.05	5.65	5.60	−0.05
34ae	5.44	5.24	−0.20	8.80	8.89	0.09	6.40	6.52	0.12	5.35	5.21	−0.14
34af	6.01	6.12	0.11	8.60	8.52	−0.08	6.93	7.16	0.23	5.94	6.08	0.14
34ag	6.83	7.00	0.17	8.95	8.92	−0.03	6.27	6.12	−0.15	6.06	6.07	0.01
34aj	7.37	7.33	−0.04	8.71	8.64	−0.07	7.40	7.35	−0.05	6.98	7.02	0.04
34al	7.33	7.21	−0.12	8.29	8.49	0.20	7.49	7.47	−0.02	7.03	7.00	−0.03
34am	6.86	6.82	−0.04	8.34	8.22	−0.12	6.66	6.75	−0.09	6.45	6.48	0.03
34an	6.32	6.28	−0.04	8.23	8.27	0.04	6.56	6.44	−0.12	6.13	6.05	−0.08

characteristics of all the individual models but is closer to PPARα and PPARγ-models which is desirable and according to our expectations.

3.3. Validation of models

Validation is the most important step in the development of reliable QSAR models, with good predictive power [43,44]. All the CoMFA models have been validated using test set of 9 compounds for which results are given in Table 4. The prediction power of the models is reasonably good except for **34k** and **34m** in case of α-model and **34x** in case of γ-model, where the residuals are greater than one log unit. These, molecules may have slightly different conformation in the active site of the respective receptors which is not a rare instance for PPAR ligands. In addition, the 'sum-model' was further validated by comparing the predicted EC_{50} from this model with the sum of predicted EC_{50} of individual models of all the molecules (last two columns of Table 4). As expected, the corresponding values in these two columns are quite comparable and thus further build the confidence in the given models. Furthermore, as discussed above, the 'sum-model' and α-model shows electrostatically unfavourable and favorable regions near R_4 and R_5, respectively. This is in accordance with the experimental findings for **34z**, **34aa**, **34ab** and **34ac** which possess a −COOH group (unfavourable) at R_4. Accordingly, these molecules are not only poorly active at PPARα but also the total EC_{50} for these is quite high. In addition, the molecule **34c** which lacks the −COOH group at R4 position but has remaining structure identical to **34ab**, is found to be around four times potent on PPARα as compared to the later, thus confirming the validity of the models.

3.4. Design of new PPAR pan ligands

The CoMFA contour maps can be exploited for the purpose of the lead optimization. We employed 'sum-model' in order to design new molecules with improved activity as compared to the most potent molecule in vitro **34p** or in vivo that is **34r**. Electrostatic contours of the 'sum-model' seem to provide major clues rather than the steric contours for the optimization of activities. All the designed molecules were then subjected to the individual α-, δ-, and γ-models for the activity prediction at individual subtypes. Thus, the sum of predicted EC_{50} at individual subtype can be compared to the EC_{50} obtained from the 'sum-model'; the model should be further validated if these two values are comparable. It should be noted that the developed 'sum-model' should give clues to improve the overall activity (sum of activities) and do so by improving activity at PPARα and PPARγ subtypes particularly.

Initial set of molecules were designed keeping in view the electrostatically favorable red contour maps around the cyclohexyl ring of **34p** (Fig. 5). Thus, the substitution of the later was done with fluorine at various positions with different stereochemistry so as to follow the red contour maps. This resulted in molecules **D1** to **D5** (Table 5) with improved overall sum of activities as compared to **34r**. The molecule **D1** was predicted to be almost equipotent to **34p**, while other

Table 4
Actual (act) and predicted (pred) pEC_{50} [M] and EC_{50} [nM] values and the residuals (Δ) of the test set molecules for the α, δ, γ and sum-models

Compd	Act pEC_{50} (α)	Pred pEC_{50} (α)	Δ	Pred EC_{50} (α)	Act pEC_{50} (δ)	Pred pEC_{50} (δ)	Δ	Pred EC_{50} (δ)	Act pEC_{50} (γ)	Pred pEC_{50} (γ)	Δ	Pred EC_{50} (γ)	Act pEC_{50} (sum)	Pred pEC_{50} (sum)	Δ	Pred EC_{50} (sum)	Pred EC_{50} ($\alpha+\delta+\gamma$)
34e	6.83	6.36	−0.47	436.5	7.96	8.21	0.25	6.2	7.35	7.69	0.34	20.4	6.69	6.58	0.11	**263.0**	**463.1**
34f	6.60	5.76	−0.84	1737.8	8.60	8.28	−0.32	5.2	7.19	6.86	−0.33	138.0	6.49	5.95	0.54	**1122.0**	**1881.0**
34k	7.08	6.00	−1.08	1000.0	8.40	8.39	−0.01	4.1	7.48	6.75	−0.73	177.8	6.92	6.12	0.80	**758.6**	**1181.9**
34m	6.48	7.60	1.12	25.1	8.46	8.33	−0.13	5.0	7.03	7.72	0.69	19.0	6.37	7.19	−0.82	**64.6**	**49.1**
34q	7.36	6.49	−0.87	322.6	8.48	8.55	0.07	2.8	7.08	6.88	−0.20	132.0	6.88	6.46	0.42	**346.7**	**457.4**
34r	6.99	7.02	0.03	95.5	8.40	8.86	0.46	1.4	7.38	7.70	0.32	20.0	6.83	6.96	−0.13	**109.6**	**116.9**
34w	6.25	5.94	−0.31	1148.2	8.47	7.96	−0.51	11.0	7.31	6.89	−0.42	128.8	6.21	5.99	0.22	**1023.3**	**1288.0**
34x	6.85	6.13	−0.72	741.3	8.36	7.55	−0.81	28.2	7.70	6.55	−1.15	281.8	6.78	5.86	0.92	**1380.4**	**1051.3**
34ah	6.98	7.48	0.50	33.1	8.70	8.77	0.07	1.7	7.39	7.58	0.19	26.3	6.83	7.10	−0.27	**79.4**	**61.1**
34ai	5.87	6.85	0.98	141.2	8.47	8.83	0.36	1.5	6.04	6.78	0.74	166.0	5.64	6.45	−0.81	**354.8**	**308.7**
34ak	6.74	6.74	0.00	182.0	8.52	8.82	0.30	1.5	7.36	6.63	−0.73	234.4	6.64	6.32	0.32	**478.6**	**417.9**

molecules were found to be lesser active compared to **34p** but highly active when compared to **34r**. Predictions with the individual models revealed that these molecules also showed improvement in activity at PPARα and PPARγ subtypes. However, as expected predicted activity at PPARδ was not affected much as compared to **34p**. In addition, the activity predicted by 'sum-model' was found to be comparable to the sum of predicted activity obtained from the individual models.

A simple substitution of 'S' with 'NH' in the thiazolyl ring of **34p** (in case of **D6**) also showed improved activity at all the subtypes as compared to **34r**. A small sterically favored green contour near R_1 in 'sum-model' was also exploited by elongating the *n*-Pr side chain with one carbon atom in **34p** (as in **D7**). This substitution led to the marked improvement in the overall activity as observed by pEC_{50} of 7.41. This is expected since this contour is reminiscent of the γ-model and is of larger size in the later. When structural features of **D6** and **D7** were combined in **D8** pEC_{50} of 7.39 was observed. Interestingly, this compound showed intermediate predicted EC_{50} values against all the receptor subtypes when compared to **D6** and **D7**.

In case of **D9**, the −NH of thiazolyl ring of **D6** was further substituted with $-CH_2COOH$ group that improved the activity for PPARα and PPARγ and the overall sum of EC_{50} but activity at PPARδ was decreased as compared to **34r**. Replacing *n*-Pr group of **34p** with *n*-propoxy group resulted in **D10** which also led to the similar effect. Further substitution of 'S' of thiazolyl ring with 'NH' in **D10** (in case of **D11**) showed the similar predicted activities as with **D9**.

More molecules were designed by substituting aromatic ring directly attached to thiazolyl ring in **34p** in order to exploit red contour map around this region. Substitution of this aromatic ring at position 5 with −F in **34p** led to **D12** with predicted EC_{50} of 7.39 from the 'sum-model'. At individual subtypes, this molecule showed activity very similar to **D8**. When the same position was substituted with −OMe, as in **D13**, it also led to the improvement of activity as compared to **34r**. This shows that both electron withdrawing and electron donating groups can be tolerated at this position. Thus, the molecules with improved overall predicted activity were designed as pan agonists using 'sum-model'. Also, the predicted activities from the 'sum-model' were found to be very close to the sum of predicted activities from the individual models for all the designed molecules (Table 5). This further validates that the 'sum-model' can predict the overall sum of activities of these molecules at all the three PPAR receptor subtypes and builds the confidence that it can be used to design such molecules.

3.5. Docking studies of designed molecules

Docking studies of all the designed molecules were performed together with the **34p** and **34r** in the PPARγ active site (PDB entry 2F4B) [20]. The molecules **34p** and **34r** were found to dock in the similar conformation and in the same binding pocket of the protein that is occupied by the co-crystallized ligand **10**, as shown in Fig. 6. This supports our earlier hypothesis of using bioactive conformation of **10**

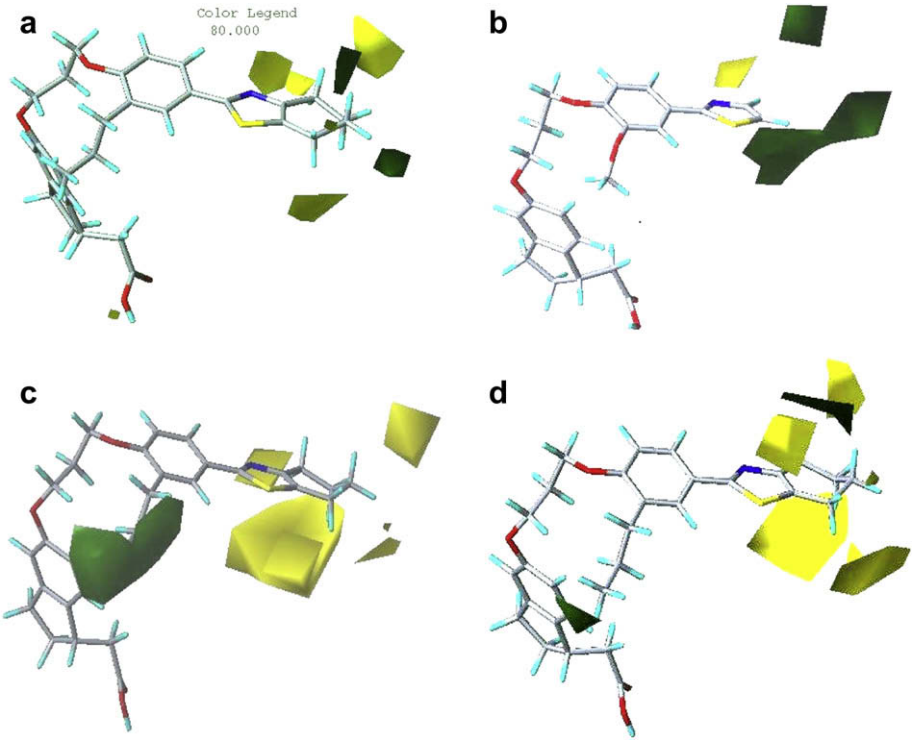

Fig. 3. Steric maps for α-model (a), δ-model (b), γ-model (c) and 'sum-model' (d).

as a template for the training set molecules for CoMFA analysis. In addition, all the designed molecules were also found to dock with similar conformation or pose with scores either better or comparable to **34p** and **34r** (Table 5) with the only exception of **D10**. The higher predicted pEC_{50} of **D6**, **D8**, and **D11** can be correlated to their docking results in the PPARγ activity. These molecules were designed by replacing the 'S' atom of the thiazolyl ring to 'NH' group, thus leading

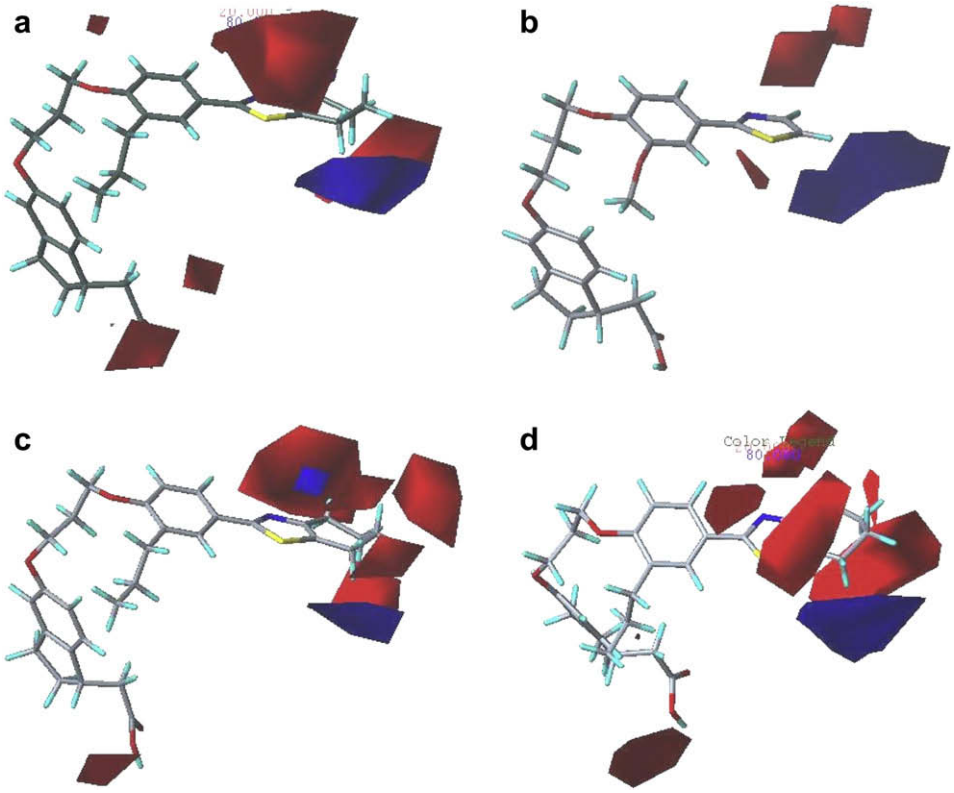

Fig. 4. Electrostatic maps for α-model (a), δ-model (b), γ-model (c) and 'sum-model' (d).

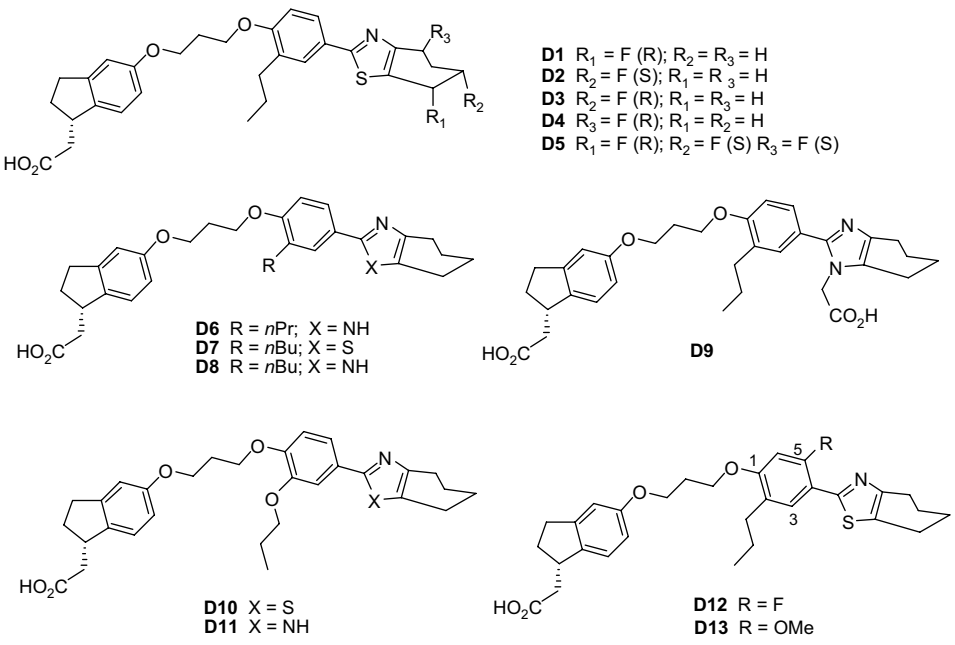

Fig. 5. Structures of molecules designed from the 'sum-model'.

to the presence of an additional hydrogen donor in the tail portion (part D, Table 1) of the molecules. This resulted in the formation of an additional H-bond with the backbone carbonyl of Ile281 (exemplified by **D8** in Fig. 6) which is absent in both **34p** and **34r**. Thus, all the designed molecules possessed better docking scores in PPARγ with respect to the most potent molecules, **34p** and **34r**, in the dataset while maintaining the vital interactions with the protein.

4. Conclusions

Manipulation of activities like multiplication and division are being used to address the problems of selectivity and duality of multiple activating agents. Similar concept has been extended in this work in designing the PPAR pan agonists. Development of these agents is very challenging as the molecules should have affinity for all the three known subtypes of PPAR (PPARα, PPARγ and PPARδ).

A reported dataset of pan agonists was used for the development of CoMFA models, where most of the molecules were shown to have potent EC_{50} values for PPARδ subtype but were only moderately potent at PPARα and PPARγ. From this data, we set our objective to develop a CoMFA model that should predict the overall activity at all the subtypes and should give clues about improving the activity at the subtypes where most of the molecules are less active. In other words the final CoMFA model should have balanced fields and should be closer to PPARα and PPARγ rather than the PPARδ in this specific case. For this purpose, a new concept based on 'sum of activities' was introduced. This approach includes the

Table 5
Predicted (pred) pEC_{50} [M], EC_{50} [nM] and docking scores of the designed molecules as compared to **34p** and **34r**

Compd	Pred (sum-model)		Pred (α-model)		Pred (δ-model)		Pred (γ-model)		Pred (α + δ + γ)	Docking Score (FlexX)
	pEC_{50}	EC_{50}	pEC_{50}	EC_{50}	pEC_{50}	EC_{50}	pEC_{50}	EC_{50}	EC_{50}	
34p	7.35	44.6	7.47	33.9	8.68	2.1	7.92	12.0	48.0	−19.8
34r	6.96	109.6	7.02	95.5	8.86	1.4	7.70	20.0	116.9	−16.7
D1	7.38	41.7	7.53	29.5	8.61	2.4	8.20	6.3	38.2	−20.7
D2	7.18	66.1	7.20	63.1	8.65	2.2	7.85	14.1	79.4	−18.7
D3	7.20	60.2	7.22	60.2	8.60	2.5	7.91	12.3	75.0	−19.0
D4	7.08	83.1	6.98	104.7	8.66	2.2	7.63	23.4	130.3	−17.7
D5	7.05	89.1	7.03	93.3	8.52	3.0	8.21	6.2	102.5	−20.8
D6	7.30	50.1	7.40	39.8	8.75	1.8	7.94	11.5	53.1	−25.9
D7	7.41	38.9	7.54	28.8	8.68	2.1	8.06	8.7	39.6	−20.4
D8	7.39	40.7	7.49	32.4	8.69	2.0	8.05	8.9	43.3	−25.3
D9	7.02	95.5	7.00	100.0	8.44	3.6	7.96	11.0	114.0	−24.9
D10	7.09	81.3	7.11	77.6	8.45	3.5	7.61	24.5	105.6	−15.4
D11	7.01	97.7	6.98	104.7	8.43	3.7	7.56	27.5	135.9	−24.4
D12	7.39	40.7	7.49	32.4	8.78	1.6	8.09	8.1	42.1	−20.6
D13	7.31	49.0	7.31	49.0	8.52	3.0	8.06	8.7	59.7	−19.6

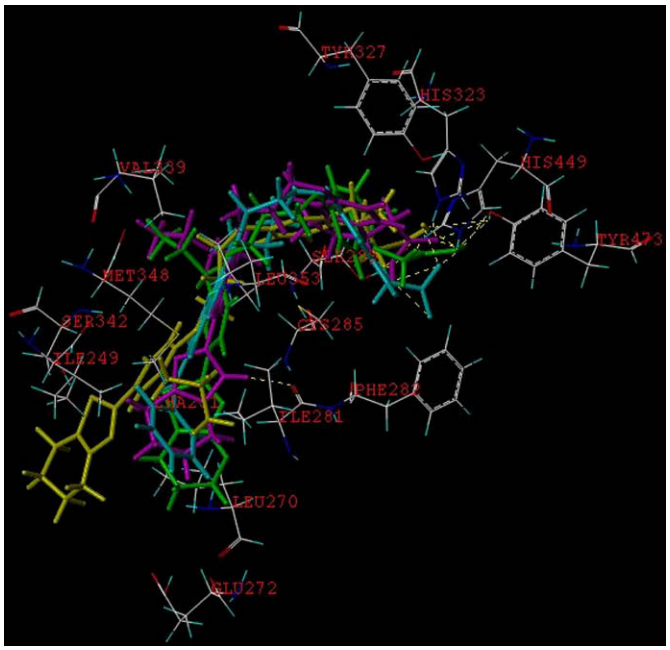

Fig. 6. The active site of PPARγ (2F4B) with important amino acid residues (shown in stick model) and various docked ligands (shown in capped stick model). The docked ligands **34p** (yellow), **34r** (green), and **D8** (magenta) bind in similar fashion as compared to the co-crystallized ligand (cyan) and make three conserved H-bonds with the His323, His449 and Tyr473. The designed molecule **D8** makes an additional H-bond with the backbone carbonyl of Ile281 owing to presence of 'NH' group in the tail portion. (For interpretation of the references to color in this figure legend, the reader is referred to the web version of this article.)

development of a CoMFA 'sum-model' that uses the numerical value obtained by adding the activities of a molecule at all three subtypes as a dependent parameter. In addition, the individual α-, δ- and γ-CoMFA models were also developed for the comparison purpose from the same set of molecules. All the models were cross-validated using the external test set of molecules. The models were found to have r^2_{cv} ranging from 0.549 to 0.757 and r^2_{ncv} ranging from 0.941 to 0.981. The predictive power of the models was sufficiently reliable with SEE values ranging from 0.097 to 0.160 for the four models. As expected the 'sum-model' was found to have similar molecular fields as in α-model and γ-model where most of the molecules are moderately active. However, it was found to possess quite different contours when compared to δ-model where most of the molecules are exhibiting potent activity. This similarity is also evident from the steric and electrostatic field contributions. Finally, the 'sum-model' was used to design new molecules with better predicted 'overall activity' and docking scores as compared to reference molecules **34p** and **34r**.

Thus, the concept of 'sum of activities' for the design of 'multiple activators' or the molecules desirable to have balanced activity on more than one target has been introduced. We have shown the application of this approach for the design of PPAR pan agonists which are the subject of current interest for the treatment of type-2 diabetes and obesity. The 'sum-model' proposed in this work provides a satisfactory result for PPAR pan agonists. This concept may also be applied for designing other known multiple activating drugs [25]. It is worth verifying the validity of this approach on many statistical model building paradigms. The current effort is to share our experience with the scientific community and prod the members to verify the validity of such approach from all possible angles. This provides an opportunity to expand the scope of QSAR models especially in the wake of limitations and predictive power discussed [43,44].

Acknowledgements

Sandeep Sundriyal gratefully acknowledges the Department of Science and Technology (DST) for providing senior research fellowship.

References

[1] Nuclear Receptors Nomenclature Committee, Cell 97 (1999) 161–163.
[2] J.P. Berger, T.E. Akiyama, P.T. Meinke, Trends Pharmacol. Sci. 26 (2005) 244–251.
[3] B.P. Kota, T.H.-W. Huang, B.D. Roufogalis, Pharm. Res. 51 (2005) 85–94.
[4] B.C.C. Cantello, M.A. Cawthorne, G.P. Cottam, P.T. Duff, D. Haigh, R.M.C.A. Hindley, S.A. Smith, P.L. Thurlby, J. Med. Chem. 37 (1994) 3977–3985.
[5] J.A. Balfour, G.L. Plosker, Drugs 57 (1999) 921–930.
[6] M.A. Peraza, A.D. Burdick, H.E. Marin, F.J. Gonzalez, J.M. Peters, Toxicol. Sci. 90 (2006) 269–295.
[7] P.H. Chong, B.S. Bachenheimer, Drugs 60 (2000) 55–93.
[8] H.J. Milionis, M.S. Elisaf, D.P. Mikhailidis, Curr. Med. Res. Opin. 16 (2000) 21–32.
[9] C. Fievet, J.-C. Fruchart, B. Staels, Curr. Opin. Pharmacol. 6 (2006) 1–9.
[10] B.R. Henke, J. Med. Chem. 47 (2004) 4118–4127.
[11] W. Oliver Jr., J.L. Shenk, M.R. Snaith, C.S. Russell, K.D. Plunket, N.L. Bodkin, M.C. Lewis, D.A. Winegar, M.L. Sznaidman, M.H. Lambert, H.E. Xu, D.D. Sternbach, S.A. Kliewer, B.C. Hansen, T.M.A. Willson, Proc. Natl. Acad. Sci. U.S.A. 98 (2001) 5306–5311.
[12] S. Luquet, C. Gaudel, D. Holst, J. Lopez-Soriano, C. Jehl-Pietri, A. Fredenrich, P.A. Grimaldi, Biochim. Biophys. Acta 1740 (2005) 313–317.
[13] T. Tanaka, J. Yamamoto, S. Iwasaki, H. Asaba, H. Hamura, Y. Ikeda, M. Watanabe, K. Magoori, R.X. Ioka, K. Tachibana, Y. Watanabe, Y. Uchiyama, K. Sumi, H. Iguchi, S. Ito, T. Dio, T. Hamakubo, M. Naito, J. Auwerx, M. Yanagisawa, T. Kodama, J. Sakai, Proc. Natl. Acad. Sci. U.S.A. 100 (2003) 15924–15929.
[14] Y.-X. Wang, C.-H. Lee, S. Tiep, R.T. Yu, J. Ham, H. Kang, R.M. Evans, Cell 113 (2003) 159–170.
[15] S. Takahashi, T. Tanaka, T. Kodama, J. Sakai, Pharmacol. Res. 53 (2006) 501–507.
[16] D. Holst, S. Luquet, V. Nogueira, K. Kristiansen, X. Leverve, P.A. Grimaldi, Biochem. Biophys. Acta 1633 (2003) 43–50.
[17] C.-H. Lee, A. Chawla, N. Urbiztondo, D. Liao, W.A. Boisvert, R.M. Evans, Science 302 (2003) 453–457.
[18] J. Rudolph, L. Chen, D. Majumdar, W.H. Bullock, M. Burns, T. Claus, F.E.D. Cruz, M. Daly, F.J. Ehrgott, J.S. Johnson, J.N. Livingston, R.W. Schoenleber, J. Shapiro, L. Yang, M. Tsutsumi, X. Ma, J. Med. Chem. 50 (2007) 984–1000.
[19] A.D. Adams, W. Yuen, Z. Hu, C. Santini, A.B. Jones, K.L. MacNaul, J.P. Berger, T.W. Doebberb, D.E. Mollerb, Bioorg. Med. Chem. Lett. 13 (2003) 931–935.
[20] N. Mahindroo, C.-F. Huang, Y.-H. Peng, C.-C. Wang, C.-C. Liao, T.-W. Lien, S.K. Chittimalla, W.-J. Huang, C.-H. Chai, E. Prakash, C.-P. Chen, T.-A. Hsu, C.-H. Peng, I.-L. Lu, L.-H. Lee, Y.W. Chang, W.-C. Chen, Y.-C. Chou, C.-T. Chen, C.M.V. Goparaju, Y.-S. Chen,

S.-J. Lan, M.-C. Yu, X. Chen, Y.-S. Chao, S.-Y. Wu, H.-P. Hsieh, J. Med. Chem. 48 (2005) 8194–8208.
[21] N. Mahindroo, C.-C. Wang, C.-C. Liao, C.-F. Huang, I.L. Lu, T.-W. Lien, Y.-H. Peng, W.-J. Huang, Y.-T. Lin, T.-A. Hsu, C.-H. Lin, C.-H. Tsai, J.T.-A. Hsu, X. Chen, P.-C. Lyu, Y.-S. Chao, S.-Y. Wu, H.-P. Hsieh, J. Med. Chem. 49 (2006) 1212–1216.
[22] J.P. Mogensen, L. Jeppesen, P.S. Bury, I. Pettersson, J. Fleckner, J. Nehlin, K.S. Frederiksen, T. Albrektsen, N. Din, S.B. Mortensen, L.A. Svensson, K. Wassermann, E.M. Wulff, L. Ynddal, P. Sauerberg, Bioorg. Med. Chem. Lett. 13 (2003) 257–260.
[23] J.J. Lin, U. Mehra, W. Wang, H.I. Krupka, C. Zhang, A. Marimuthu, B. Powell, C.R. Hurt, P.N. Ibrahim, D.R. Artis, M.V. Milburn, Abstracts of Papers, 227th ACS National Meeting, Anaheim, USA, 2004, MEDI-225.
[24] <http://www.plexxicon.com> (accessed 23.10.07).
[25] R. Morphy, Z. Rankovic, J. Med. Chem. 48 (2005) 6523–6543.
[26] G. Wong, K.F. Koehler, P. Skolnick, Z.Q. Gu, S. Ananthan, P. Schonholzer, W. Hunkeler, W. Zhang, J.M. Cook, J. Med. Chem. 36 (1993) 1820–1830.
[27] I.I. Baskin, I.G. Tikhonova, V.A. Palyuin, N.S. Zefirov, J. Med. Chem. 46 (2003) 4063–4069.
[28] S. Khanna, M.E. Sobhia, P.V. Bharatam, J. Med. Chem. 48 (2005) 3015–3025.
[29] N. Dessalew, P.V. Bharatam, Eur. J. Med. Chem. 42 (2007) 1014–1027.
[30] L. Rathi, S.K. Kashaw, A. Dixit, G. Pandey, A.K. Saxena, Bioorg. Med. Chem. 12 (2004) 63–69.
[31] A. Dixit, A.K. Saxena, Eur, J. Med. Chem 43 (2008) 73–80.
[32] C. Liao, A. Xie, L. Shi, J. Zhou, X. Lu, J. Chem. Inf. Comput. Sci. 44 (2004) 230–238.
[33] K.H. Hyun, D.Y. Lee, B.-S. Lee, C.K. Kim, QSAR Comb. Sci. 23 (2004) 637–649.
[34] C. Liao, A. Xie, J. Zhou, L. Shi, Z. Li, X.-P. Lu, J. Mol. Model. 10 (2004) 165–177.
[35] C. Rucker, M. Scarsi, M. Meringer, Bioorg. Med. Chem. 14 (2006) 5178–5195.
[36] SYBYL6.9, Tripos Inc., 1699 S. Hanley Rd., St. Louis, MO 631444, USA.
[37] J. Bostrom, A. Hogner, S. Schmitt, J. Med. Chem. 49 (2006) 6716–6725.
[38] R.T. Nolte, B.G. Wisley, S. Westin, J.E. Cobb, M.H. Lambert, R. Kurokawa, M. Rosenfeld, Nature 395 (1998) 137–143.
[39] J.J.P. Stewart, J. Comput. Aided Mol. Des. 4 (1990) 1–105.
[40] M. Rarey, B. Kramer, T. Lengauer, G.J. Klebe, Mol. Biol. 261 (1996) 470–489.
[41] H. Koyama, J.K. Boueres, W. Han, E.J. Metzger, J.P. Bergman, D.F. Gratale, D.J. Miller, R.L. Tolman, K.L. MacNaul, J.P. Berger, T.W. Doebber, K. Leung, D.E. Moller, J.V. Heck, S.P. Sahoo, Bioorg. Med. Chem. Lett. 13 (2003) 1801–1804.
[42] R.C. Desai, W. Han, E.J. Metzger, J.P. Bergman, D.F. Gratale, K.L. MacNaul, J.P. Berger, T.W. Doebber, K. Leung, D.E. Moller, J.V. Heck, S.P. Sahoo, Bioorg. Med. Chem. Lett. 13 (2003) 2795–2798.
[43] A. Golbrakikh, A. Tropsha, J. Mol. Graph. Model. 20 (2002) 269–276.
[44] A. Tropsha, in: T.I. Opera (Ed.), Chemoinformatics in Drug Discovery, vol. 22, Wiley-VCH, Weinheim, 2004, pp. 437–455.